Available online at www.sciencedirect.com
ScienceDirect
Tunnelling and Underground Space Technology 23 (2008) 588–599
Tunnelling and Underground Space Technology incorporating Trenchless Technology Research
www.elsevier.com/locate/tust

A new numerical procedure for elasto-plastic analysis of a circular opening excavated in a strain-softening rock mass

Youn-Kyou Lee [a,*], S. Pietruszczak [b]

[a] Department of Ocean System Engineering, Kunsan National University, Miryong-Dong, Gunsan, Jeonbuk 573-701, Republic of Korea
[b] Department of Civil Engineering, McMaster University, 1280 Main Street West, Hamilton, Ont., Canada L8S 4L7

Received 26 July 2007; received in revised form 6 November 2007; accepted 9 November 2007
Available online 20 December 2007

Abstract

A simple numerical procedure for calculating the distribution of stresses and radial displacements around a circular tunnel excavated in a strain-softening Mohr–Coulomb or generalized Hoek–Brown rock mass is proposed. The problem is considered as axisymmetric, i.e. the initial stress state is assumed to be hydrostatic and the rock mass is said to be isotropic. By invoking the finite difference approximation of the equilibrium and compatibility equations, the increments of stresses and strains for each ring, starting from the outmost one for which boundary conditions are known a priori, are calculated in a successive manner. In the proposed approach, the potential plastic zone is divided into a finite number of concentric rings whose thicknesses are determined internally to satisfy the equilibrium equation. For the strain-softening behavior, it is assumed that all the strength parameters are a linear function of deviatoric plastic strain. Several illustrative examples are given to demonstrate the performance of the proposed method. For the brittle–plastic case, the results show a very good agreement with the closed-form solution. For strain-softening cases, the predictions by the proposed method are also in good agreement with the known rigorous numerical solutions. It is shown that the approximate solution converges to the exact solution when the increment of stress for each ring becomes smaller. The influence of the strength parameter 'a', appearing in the generalized Hoek–Brown criterion, on the elasto-plastic solutions is examined through the establishment of ground reaction curves and the discussion for the locations of the plastic radii.

Keywords: Strain-softening; Hoek–Brown criterion; Mohr–Coulomb criterion; Elasto-plastic analysis; Axisymmetric problem; Circular opening

1. Introduction

Analysis of stresses and displacements around circular opening excavated in isotropic rock masses has been one of the fundamental problems in geotechnical engineering. Provided that the initial stress field is hydrostatic, the problem may be regarded as axisymmetric and an analytical solution can be found. This solution is useful in various situations that include the validation of constitutive models, the stability assessments of circular openings such as borehole and TBM excavated tunnel, the verification of numerical codes, the construction of ground-support reaction curves, etc. In general, a reliable solution requires a nonlinear approach, because the deformation response depends on the stress path. According to the existing literature surveys (Brown et al., 1983; Alonso et al., 2003), elasto-plastic approaches seem to be most popular.

In the past, Mohr–Coulomb (M–C) yield criterion was the most common in the elasto-plastic analysis of rock mass, due to its simplicity. However, experimental observations show that the strength envelope for most of rock-like materials is not linear. Among the nonlinear yield criteria, the criterion by Hoek and Brown (1980) is widely accepted in rock mechanics community, as it provides a reliable tool for predicting the strength of jointed rock mass. Recently

* Corresponding author. Tel.: +82 63 469 1864; fax: +82 63 463 9493.
E-mail address: kyoulee@kunsan.ac.kr (Y.-K. Lee).

0886-7798/$ - see front matter © 2007 Elsevier Ltd. All rights reserved.
doi:10.1016/j.tust.2007.11.002

Hoek–Brown (H–B) criterion has been updated to the generalized form (Hoek et al., 2002), in which the strength parameter 'a' is no longer constant and can vary from 0.5 for the excellent rock mass having GSI = 100 to 0.6 for the very poor rock mass of GSI = 10.

Elasto-plastic analysis of circular tunnels excavated in H–B or M–C media was attempted by many researchers. Although a number of closed-form solutions are available, each solution is approximate, in the sense that it incorporates various simplifying assumptions. For elastic–brittle–plastic case, Brown et al. (1983) presented the closed-form solution for stress and radial displacement in the plastic zone. However, they did not consider the variation of elastic strain, so that the influence of the unloading in the plastic zone is not taken into account. In addition, Brown et al.'s solution has a defect in predicting the plastic radius as pointed out by Wang (1996). Recently, improved solutions were provided by several authors. While Carranza-Torres and Fairhurst (1999) solution for H–B rock mass, which is based on the so-called self-similarity of H–B criterion, is theoretically rigorous, it seems rather complicated for practical use and it is applicable only to the elastic–perfectly plastic case. An analytical solution for H–B rock mass given by Sharan (2003) is also not exact in calculating displacements in plastic zone, as it assumes that the elastic strain field in the plastic zone is the same as that of thick-wall cylinder problem (Timoshenko and Goodier, 1982). On the other hand, solutions by Park and Kim (2006) and Carranza-Torres (2004) give an exact expression for displacement in the plastic zone. However, even for elastic–brittle–plastic behavior of H–B rock mass, there is no closed-form solution if the strength parameter 'a' is not equal to 0.5.

Most of elasto-plastic solutions mentioned above are relevant to elastic–perfectly plastic or elastic–brittle–plastic material. For strain-softening rock masses the attempts at elasto-plastic analysis are limited (cf. Brown et al., 1983; Duncan Fama et al., 1995; Alonso et al., 2003; Guan et al., 2007). This may be due to the difficulty in defining the material behavior and in obtaining the closed-form solutions. Although Brown et al. (1983) obtained the ground reaction curve (GRC) for a circular tunnel in a strain-softening H–B rock mass, it underestimated the convergence by neglecting the variation of elastic strain in plastic zone. On the other hand, the methodology followed by Alonso et al. (2003) for obtaining GRC for stain-softening rock masses is sound from a theoretical point of view; it seems however too complex for practical use. Guan et al. (2007) compared the radial displacements from the rigorous methods (Alonso et al., 2003) with those from the simplified method (Brown et al., 1983) and reported that, when Brown et al.'s method is used, the prediction error in the radial displacement is in the range of 20–40%. Those current rigorous solutions for the strain-softening behavior, however, are doubtful whether they are practical, because they require solving rather complicated second order differential equations (Carranza-Torres, 1998; Guan et al., 2007) or a system of differential equations (Alonso et al., 2003).

This paper proposes a simple and practical numerical procedure to calculate the distribution of displacements and stresses around circular opening excavated in isotropic strain softening rock masses. The discussion of this paper is restricted to the stable basic solution in the strain-softening zone, so the topics concerning the instability such as bifurcation and strain localization in the strain-softening regime (Varas et al., 2005) is not addressed. The proposed model is formulated in a unified manner to accommodate both the M–C and generalized H–B rock masses. By assuming that initial stress field is hydrostatic, the analysis simplifies to axisymmetric conditions. In the post-failure state, all the strength parameters are assumed to be a function of deviatoric plastic strain and to decrease linearly to the residual values. In the model, the plastic strains are calculated incrementally and the plastic flow rule can be associated or non-associated. The potential plastic zone is subdivided into a sufficiently large number of concentric annuli whose thicknesses are not uniform but determined internally to comply with the equilibrium equation. Since the radial stress, which is a minor principal stress for this axisymmetric problem, is known on both the elastic–plastic interface and the excavation boundary, the increments of plastic strains are obtained successively through finite difference approximation of equilibrium and compatibility equations in each plastic ring, starting from the outmost one. The validity and potential for practical use of the proposed method is demonstrated through a number of illustrative examples. Since elastic–brittle–plastic cases are special cases of strain-softening behavior and many closed-form solutions exist, some elastic–brittle–plastic solutions are compared with the results form the proposed method. Some published rigorous strain-softening solutions are also reproduced by use of the proposed method to demonstrate the validity of the model.

2. Definition of problem

Fig. 1 shows a circular tunnel of radius b excavated in an infinite isotropic rock mass. Here, a hydrostatic stress field σ_0 is imposed throughout the domain before the excavation takes place. When the internal support pressure p_i is lower than a critical value p_{ic}, a plastic zone may be formed around the opening. In the case of elastic–brittle–plastic or elastic–perfectly plastic behavior, it is possible to derive an explicit expression for the plastic radius R_p (Carranza-Torres and Fairhurst, 1999; Park and Kim, 2006). On the other hand, if strain-softening behavior is considered, the plastic zone may be divided into softening and residual zones by an interface whose radius is denoted by R_s, shown in Fig. 1. In this case, no closed-form solution is available and the plastic/softening radius, as well as the distributions of stresses and displacements in plastic zone, should be assessed numerically.

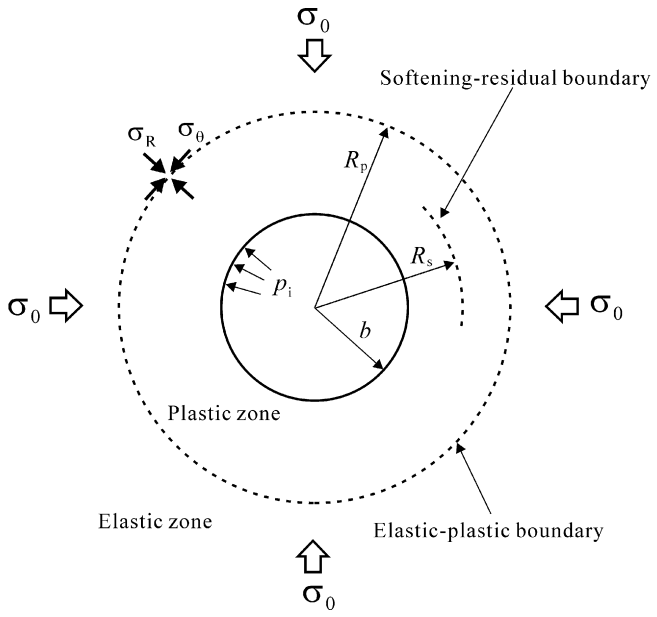

Fig. 1. Plastic zone formed around circular opening.

2.1. Yield function

It is assumed that the yielding of the rock mass is governed by the yielding function,

$$F(\sigma_\theta, \sigma_r, \gamma^{\mathrm{p}}) = \sigma_\theta - \sigma_r - H(\sigma_r, \gamma^{\mathrm{p}}) \tag{1}$$

where σ_θ and σ_r are the major and minor principal stresses, respectively, whereas γ^{p} is the strain-softening parameter controlling the evolution of the strength parameters in the strain-softening regime and defined as the following deviatoric plastic strain:

$$\gamma^{\mathrm{p}} = \gamma_\theta^{\mathrm{p}} - \gamma_r^{\mathrm{p}} \tag{2}$$

Although there is no universal way of defining the strain-softening parameter as pointed out by Alonso et al. (2003), the definition of Eq. (2) is most widely accepted.

For M–C rock mass, H in Eq. (1) becomes

$$H^{\mathrm{MC}}(\sigma_r, \gamma^{\mathrm{p}}) = (N(\gamma^{\mathrm{p}}) - 1)\sigma_r + Y(\gamma^{\mathrm{p}}) \tag{3}$$

where N and Y are strength parameters defined in terms of friction angle $\phi(\gamma^{\mathrm{p}})$ and cohesion $c(\gamma^{\mathrm{p}})$;

$$N(\gamma^{\mathrm{p}}) = \frac{1+\sin\phi(\gamma^{\mathrm{p}})}{1-\sin\phi(\gamma^{\mathrm{p}})}; \quad Y(\gamma^{\mathrm{p}}) = \frac{2c(\gamma^{\mathrm{p}})\cos\phi(\gamma^{\mathrm{p}})}{1-\sin\phi(\gamma^{\mathrm{p}})} \tag{4}$$

On the other hand, if the generalized H–B yield function is assumed, H can be expressed as

$$H^{\mathrm{HB}}(\sigma_r, \gamma^{\mathrm{p}}) = \sigma_{\mathrm{c}}(\gamma^{\mathrm{p}})\left(m(\gamma^{\mathrm{p}})\frac{\sigma_r}{\sigma_{\mathrm{c}}(\gamma^{\mathrm{p}})} + s(\gamma^{\mathrm{p}})\right)^{a(\gamma^{\mathrm{p}})} \tag{5}$$

where σ_{c} is the uniaxial compressive strength of rock, and m, s, and a are the strength parameters of H–B criterion.

2.2. Plastic potential function

Here, Mohr–Coulomb type of criterion is selected as a plastic potential function, so that the plastic potential function may be written as

$$G(\sigma_\theta, \sigma_r, \gamma^{\mathrm{p}}) = \sigma_\theta - k(\gamma^{\mathrm{p}})\sigma_r \tag{6}$$

where $k(\gamma^{\mathrm{p}})$ is known as the coefficient of dilation and defined as

$$k(\gamma^{\mathrm{p}}) = \frac{1+\sin\varphi(\gamma^{\mathrm{p}})}{1-\sin\varphi(\gamma^{\mathrm{p}})} \tag{7}$$

φ in Eq. (7) is so-called angle of dilation. When φ is equal to internal frictional angle ϕ of rock, the plastic flow rule is associated. If $k(\gamma^{\mathrm{p}}) = 1.0$, no plastic volume change takes place during yielding.

Then the plastic flow rule gives the following relation between the radial and circumferential plastic strain increments:

$$\mathrm{d}\varepsilon_r^{\mathrm{p}} = -k(\gamma^{\mathrm{p}})\,\mathrm{d}\varepsilon_\theta^{\mathrm{p}} \tag{8}$$

2.3. Evolution of strength parameters

It should be noted that each strength parameter appearing in Eqs. (3), (5) and (6) is a function of γ^{p}. In plastic regime, it is assumed that those parameters can be described by bilinear functions of deviatoric plastic strain γ^{p} as shown in Fig. 2,

$$\omega(\gamma^{\mathrm{p}}) = \begin{cases} \omega_{\mathrm{p}} - (\omega_{\mathrm{p}} - \omega_{\mathrm{r}})\frac{\gamma^{\mathrm{p}}}{\gamma^{\mathrm{p}^*}}, & 0 < \gamma^{\mathrm{p}} < \gamma^{\mathrm{p}^*} \\ \omega_{\mathrm{r}}, & \gamma^{\mathrm{p}} \geqslant \gamma^{\mathrm{p}^*} \end{cases} \tag{9}$$

where ω represents one of ϕ, c, σ_{c}, m, s, φ and a. γ^{p^*} is the critical deviatoric plastic strain from which the residual behavior starts and should be identified by experiments. While different γ^{p^*} may be assigned for each parameter provided that the experimental data are available, here for simplicity single value of γ^{p^*} is assumed for each medium. The subscripts 'p' and 'r' denote the peak and residual values, respectively. It should be noted that in general $a_{\mathrm{r}} \geqslant a_{\mathrm{p}}$ for the parameter a of Eq. (5). If $\gamma^{\mathrm{p}^*} = \infty$, the elastic–perfectly plastic model is retrieved, whereas Eq. (9) reduces to the elastic–brittle plastic model provided that $\omega_{\mathrm{r}} \neq \omega_{\mathrm{p}}$ and no softening behavior is allowed.

2.4. Critical supporting pressure, p_{ic}

The plastic zone around the circular opening is formed only when the internal support pressure p_{i} is lower than a

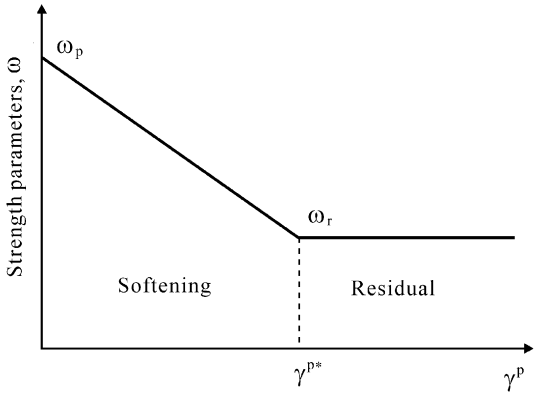

Fig. 2. Evolution of strength parameters in plastic regime.

critical value p_{ic}. For M–C rock mass, p_{ic} can be calculated by use of the peak strength parameters and the initial stress σ_0 (Brady and Brown, 1993),

$$p_{ic}^{MC} = \frac{2\sigma_0 - Y_p}{N_p + 1} \tag{10}$$

where $Y_p = 2c_p \cos\phi_p/(1 - \sin\phi_p)$ and $N_p = (1 + \sin\phi_p)/(1 - \sin\phi_p)$.

For H–B rock mass, p_{ic} can be obtained by solving the following nonlinear equation:

$$2(\sigma_0 - p_{ic}) = \sigma_{cp}\left(m_p \frac{p_{ic}}{\sigma_{cp}} + s_p\right)^{a_p} \tag{11}$$

The analytical expression for p_{ic} is available only when $a_p = 0.5$ (Carranza-Torres and Fairhurst, 1999; Park and Kim, 2006), which is

$$p_{ic}^{HB} = \frac{1}{2}\left(\beta - \sqrt{\beta^2 + 4\beta\sigma_0 + s_p\sigma_{cp}^2}\right) + \sigma_0 \tag{12}$$

where $\beta = (m_p\sigma_{cp})/4$. If $a_p > 0.5$, p_{ic}^{HB} can be found numerically by use of suitable root-finding algorithm such as Newton–Raphson method (Press et al., 1992).

It should be noted that when the plastic zone is formed, the radial stress σ_R, acting on the elastic–plastic interface (see Fig. 1), is equal to p_{ic};

$$\sigma_R = \sigma_r(R_p) = p_{ic} \tag{13}$$

It is interesting to note that σ_R is independent of radius r.

3. Approximation of strain-softening behavior

3.1. Preliminaries

It is assumed that the plastic zone is composed of n concentric annuli as shown in Fig. 3, where ith annulus is bounded by two circles of normalized radii $\rho_{(i-1)} = r_{(i-1)}/R_p$ and $\rho_{(i)} = r_{(i)}/R_p$. Here, it should be noted that the thickness of each annulus is not equal in general because it is determined automatically during the numerical process to satisfy the equilibrium condition as explained later in this section.

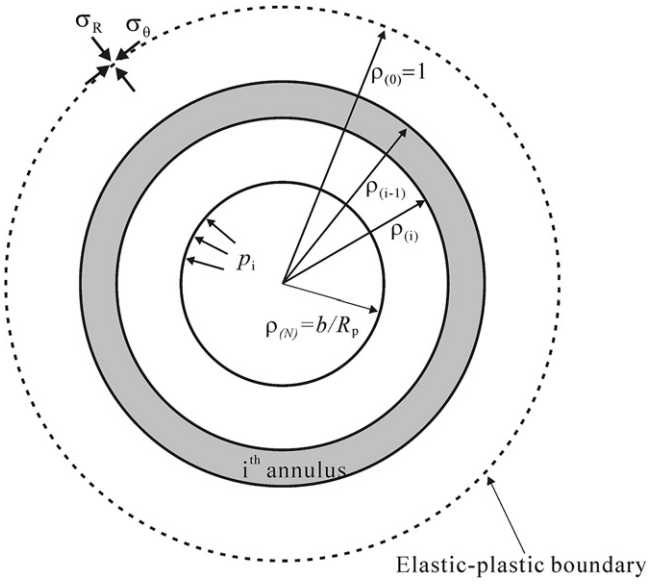

Fig. 3. Normalized plastic zone with finite number of annuli.

On the outer boundary of plastic zone, where $\rho_{(0)} = 1$, stress and strain components under plane strain condition are given as (Brown et al., 1983),

$$\begin{Bmatrix} \sigma_{r(0)} \\ \sigma_{\theta(0)} \end{Bmatrix} = \begin{Bmatrix} \sigma_R \\ 2\sigma_0 - \sigma_R \end{Bmatrix} \tag{14}$$

$$\begin{Bmatrix} \varepsilon_{r(0)} \\ \varepsilon_{\theta(0)} \end{Bmatrix} = \frac{1+\nu}{E}\begin{Bmatrix} \sigma_R - \sigma_0 \\ \sigma_0 - \sigma_R \end{Bmatrix} \tag{15}$$

where ν is Poisson's ratio and E is Young's modulus.

3.2. Increments of stresses and elastic strains

Here, the drawback in Brown et al.'s (1983) method, where the simplified assumption for the distribution of elastic strain is made, is overcome by noting the fact that σ_r on both inner and outer boundaries of the plastic zone are known *a priori* and σ_r decreases monotonically from σ_R at $r = R_p$ to p_i at $r = b$. We can take the radial stress increment

$$\Delta\sigma_r = \frac{p_i - \sigma_R}{n} \tag{16}$$

so that the stress components for ith radius may be approximated as

$$\sigma_{r(i)} = \sigma_{r(i-1)} + \Delta\sigma_r \tag{17}$$

Here, again, it should be noted that, although the constant increment of $\Delta\sigma_r$ is assumed for each annulus, the actual thickness of the annuli is not constant because the radii of annuli are to be determined to satisfy the equilibrium equation (see Eq. 24).

For a sufficiently large n, the corresponding hoop stress is given by

$$\sigma_{\theta(i)} = \sigma_{r(i)} + H(\sigma_{r(i)}, \gamma^p_{(i-1)}) \tag{18}$$

where H is defined in Eq. (3) or Eq. (5).

Thus,

$$\Delta\sigma_{\theta(i)} = \sigma_{\theta(i)} - \sigma_{\theta(i-1)} \tag{19}$$

Elastic strain increments can be related to the stress increments using Hooke's law. Under plane strain condition, there is

$$\begin{Bmatrix} \Delta\varepsilon^e_{r(i)} \\ \Delta\varepsilon^e_{\theta(i)} \end{Bmatrix} = \frac{1+\nu}{E}\begin{bmatrix} 1-\nu & -\nu \\ -\nu & 1-\nu \end{bmatrix}\begin{Bmatrix} \Delta\sigma_{r(i)} \\ \Delta\sigma_{\theta(i)} \end{Bmatrix} \tag{20}$$

3.3. Approximation of displacements

Provided that the number of annuli n is sufficiently large, the equilibrium equation expressed with respect to the normalized radius $\rho = r/R_p$,

$$\frac{d\sigma_r}{d\rho}+\frac{\sigma_r-\sigma_\theta}{\rho}=0 \tag{21}$$

or

$$\frac{d\sigma_r}{d\rho}-\frac{H(\sigma_r,\gamma^p)}{\rho}=0 \tag{22}$$

may be approximated for the ith annulus as

$$\frac{\sigma_{r(i)}-\sigma_{r(i-1)}}{\rho_{(i)}-\rho_{(i-1)}}-\frac{2H(\bar{\sigma}_{r(i)},\gamma^p_{(i-1)})}{\rho_{(i)}+\rho_{(i-1)}}=0 \tag{23}$$

where $\bar{\sigma}_{r(i)}=(\sigma_{r(i)}+\sigma_{r(i-1)})/2$.

The normalized inner radius $\rho_{(i)}=r_{(i)}/R_p$ is then expressed explicitly as

$$\rho_{(i)}=\frac{2H(\bar{\sigma}_{r(i)},\gamma^p_{(i-1)})+\Delta\sigma_r}{2H(\bar{\sigma}_{r(i)},\gamma^p_{(i-1)})-\Delta\sigma_r}\rho_{(i-1)} \tag{24}$$

In order to calculate the plastic strain increments, the displacement compatibility equation can be evoked. Since the strain components are related to the radial displacement u by

$$\varepsilon_r=\frac{du}{dr},\quad \varepsilon_\theta=\frac{u}{r} \tag{25}$$

the compatibility equation can be stated as (Florence and Schwer, 1978)

$$\frac{d\varepsilon_\theta}{d\rho}+\frac{\varepsilon_\theta-\varepsilon_r}{\rho}=0 \tag{26}$$

In the plastic zone, the total strains can be decomposed into elastic and plastic parts as follows:

$$\begin{Bmatrix}\varepsilon_r\\ \varepsilon_\theta\end{Bmatrix}=\begin{Bmatrix}\varepsilon^e_r\\ \varepsilon^e_\theta\end{Bmatrix}+\begin{Bmatrix}\varepsilon^p_r\\ \varepsilon^p_\theta\end{Bmatrix} \tag{27}$$

so that Eq. (26) can be reformulated as

$$\frac{d\varepsilon^p_\theta}{d\rho}+\frac{\varepsilon^p_\theta-\varepsilon^p_r}{\rho}=-\frac{d\varepsilon^e_\theta}{d\rho}-\frac{\varepsilon^e_\theta-\varepsilon^e_r}{\rho} \tag{28}$$

or

$$\frac{d\varepsilon^p_\theta}{d\rho}+\frac{\varepsilon^p_\theta-\varepsilon^p_r}{\rho}=-\frac{d\varepsilon^e_\theta}{d\rho}-\frac{1+\nu}{E}\frac{H(\sigma_r,\gamma^p)}{\rho} \tag{29}$$

Approximating the differential equation (29) with respect to ρ and rearranging for $\Delta\varepsilon^p_{\theta(i)}$ gives, in view of Eqs. (8), (20) and (24),

$$\left(\frac{1}{\Delta\rho_{(i)}}+(1+k_{(i-1)})\frac{1}{\bar{\rho}_{(i)}}\right)\Delta\varepsilon^p_{\theta(i)}=-\frac{\Delta\varepsilon^e_{\theta(i)}}{\Delta\rho_{(i)}}-\frac{(1+\nu)}{E}\frac{H(\bar{\sigma}_{r(i)},\gamma^p_{(i-1)})}{\bar{\rho}_{(i)}}-\frac{1}{\bar{\rho}_{(i)}}\left(\varepsilon^p_{\theta(i-1)}-\varepsilon^p_{r(i-1)}\right) \tag{30}$$

where $\bar{\rho}_{(i)}=(\rho_{(i-1)}+\rho_{(i)})/2$ and $k_{(i-1)}=(1+\sin\varphi_{(i-1)})/(1-\sin\varphi_{(i-1)})$. Corresponding $\Delta\varepsilon^p_{r(i)}$ is then given by Eq. (8). The deviatoric plastic shear strain is updated as

$$\gamma^p_{(i)}=\gamma^p_{(i-1)}+(\Delta\varepsilon^p_{\theta(i)}-\Delta\varepsilon^p_{r(i)}) \tag{31}$$

Now, the total strain at ith annulus is obtained as

$$\begin{Bmatrix}\varepsilon_{r(i)}\\ \varepsilon_{\theta(i)}\end{Bmatrix}=\begin{Bmatrix}\varepsilon_{r(i-1)}\\ \varepsilon_{\theta(i-1)}\end{Bmatrix}+\begin{Bmatrix}\Delta\varepsilon^e_{r(i)}\\ \Delta\varepsilon^e_{\theta(i)}\end{Bmatrix}+\begin{Bmatrix}\Delta\varepsilon^p_{r(i)}\\ \Delta\varepsilon^p_{\theta(i)}\end{Bmatrix} \tag{32}$$

Recalling the relation $\varepsilon_\theta=u/r$, the displacement normalized by plastic radius R_p may be calculated using the relation,

$$U_{(i)}=\varepsilon_{\theta(i)}\rho_{(i)} \tag{33}$$

where $U_{(i)}=u_{(i)}/R_p$.

If the procedure explained in above Sections 3.1 and 3.3 can be repeated n times, the last $\sigma_{r(i)}$, i.e. $\sigma_{r(n)}$, reaches the internal support pressure value p_i which is acting on the excavation surface of the opening with radius b. The plastic radius R_p can be obtained from the following relation:

$$R_p=\frac{b}{\rho_{(n)}} \tag{34}$$

Then, the radial displacement at each location can be calculated from the normalized radial displacement $U_{(i)}$, Eq. (33), as

$$u_{(i)}=U_{(i)}R_p \tag{35}$$

According to the procedure explained, it is evident that the solution will converge to the exact solution by increasing the division number n. The sequence of calculations is summarized in Appendix A.

Although the proposed finite difference approximate scheme looks similar to that from Brown et al. (1983), the procedure is completely different from Brown et al.'s at the following points of view:

- In Brown et al.'s, they assume that the elastic strain is uniform and constant over the plastic zone and calculate $\varepsilon_{\theta(i)}$, $\varepsilon_{r(i)}$, $\rho_{(i)}$, $\sigma_{r(i)}$, and $\sigma_{\theta(i)}$ in that order after selecting an arbitrary small value for $\Delta\varepsilon^p_{\theta(i)}$ in each step. Due to this simplified assumption on the distribution of elastic strain in the plastic zone, their procedure underestimates the displacement field around an opening. On the contrary, our approach starts each step with $\Delta\sigma_r$, then $\sigma_{r(i)}$, $\sigma_{\theta(i)}$, $\rho_{(i)}$, $\varepsilon_{\theta(i)}$, and $\varepsilon_{r(i)}$ are updated successively, so that the calculation in each step proceeds in reverse order of Brown et al.'s. Since the small stress increment for each annulus is assumed first, our approach calculates the increment of elastic strain for the annulus correctly by use of Hooke's law. Furthermore the increment of plastic strain is also calculated correctly by invoking the compatibility relation.
- While ρ_i in Brown et al.'s is calculated through the finite difference approximation of the strain–displacement relation, ρ_i in this study is determined by the finite difference approximation of the stress equilibrium equation.
- While Brown et al. employed ε^p_θ as a softening parameter that control the evolution of the strength parameters, our procedure selects the deviatoric plastic strain, $(\varepsilon^p_\theta-\varepsilon^p_r)$, as the softening parameter which is more widely accepted.

- Mohr–Coulomb and Hoek–Brown criteria are considered in a single framework of approximation.
- The generalized Hoek–Brown criterion is taken into account in our approach.

4. Verification examples

4.1. Verifications for H–B rock mass

4.1.1. Elastic–brittle–plastic behavior for Hoek–Brown rock mass with $a_p = a_r = 0.5$

To investigate how the results are influenced by the magnitude of $\Delta\sigma_r$ in Eq. (16), i.e. the number of annuli n, an elastic–brittle–plastic analysis was performed for which closed-form or numerical solutions are available, e.g. Park and Kim (2006) or Carranza-Torres (2004).

One of the data sets appearing in Sharan (2003) was taken as input data: $b = 5$ m, $\sigma_0 = 30$ MPa, $p_i = 5$ MPa, $E = 5.5$ GPa, $\nu = 0.25$, $\sigma_{cp} = \sigma_{cr} = 30$ MPa, $m_p = 1.7$, $s_p = 0.0039$, $m_r = 1.0$, $s_r = 0.0$, $a_p = a_r = 0.5$. Two dilation angles, $\varphi_r = 0°$ and 30°, were considered in order to examine the influence of plastic volume change. Five values of n considered in this example are 20, 50, 100, 200 and 500.

In Fig. 4, percentage errors occurring in the course of approximating radial displacements u are plotted against the normalized radius r/b in the plastic zone. Prediction errors arising from Sharan's (2003) approximation formula are also plotted for the purpose of comparison. In this case, it was calculated that $r/b = 1.885$ at the elastic–plastic interface. The positive errors can be justified when considering the fact that the explicit scheme is used in approximating the strength parameters. It is evident from the figure that the larger the value of n, the better the approximation. Even though a general guideline for selecting suitable n is not available, it seems that choosing n in the range of hundreds can give a very accurate prediction of radial displacements.

For $n = 500$, $(u - u_{exact})/u_{exact}$ is only 0.225% on the excavation surface, at $r/b = 1.0$, when the rock is non-dilatant ($\varphi_r = 0°$). However, the corresponding value increases to 0.721% when $\varphi_r = 30°$. This trend also prevails for smaller values of n, Fig. 4. Thus, the results suggest that the dilatancy effect may decrease the approximation accuracy of u and larger value of n should be used for dilating rock masses. For non-dilating rock, Fig. 4a shows that while Sharan's approximating formula gives the exact values of radial displacements at the excavation surface and at the elastic–plastic interface, the error is increased toward the interior points. For dilating rock, however, the error occurred even at the excavation surface. Although Sharan (2003) concluded that the error is maximum at the boundary of the opening, his conclusion might not be correct when considering Fig. 4b, where the maximum error occurs at an interior point of the plastic zone.

As can be seen in Fig. 5a, the distributions of stress for $n = 500$ shows good agreement with the exact solutions.

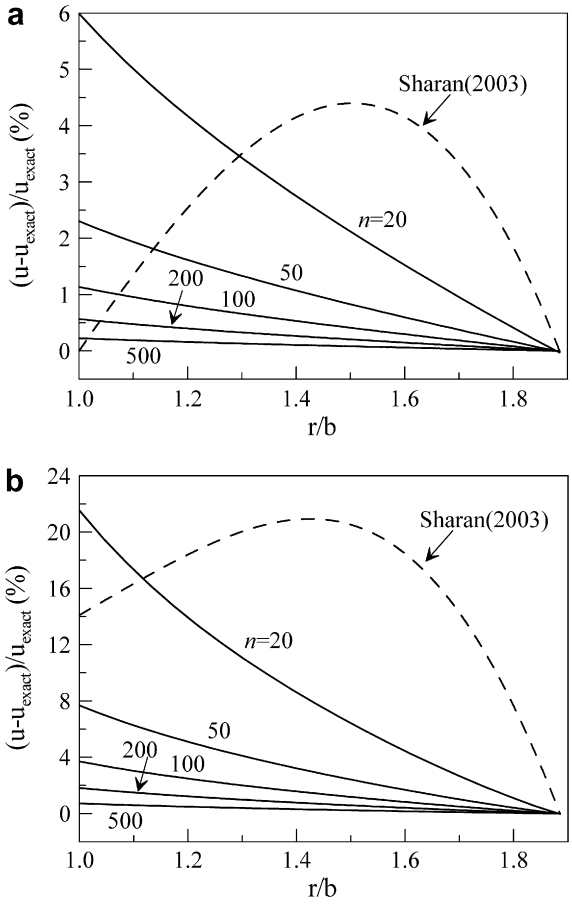

Fig. 4. Approximation errors in radial displacements for a circular opening excavated in Hoek–Brown rock mass; $b = 5$ m, $\sigma_0 = 30$ MPa, $p_i = 5$ MPa, $E = 5.5$ GPa, $\nu = 0.25$, $\sigma_{cp} = \sigma_{cr} = 30$ MPa, $m_p = 1.7$, $s_p = 0.0039$, $m_r = 1.0$, $s_r = 0.0$, $a_p = a_r = 0.5$: (a) $\varphi_r = 0°$; (b) $\varphi_r = 30°$.

The radial displacements for $n = 500$ are also plotted and compared with the exact ones in Fig. 5b along with those predicted by Brown et al. (1983) and Sharan (2003). The distribution of radial displacements calculated using the proposed methodology again shows a very good agreement with the exact solution, while Sharan's approximation is overestimating the displacements and Brown et al.'s (1983) is underestimating the displacements.

4.1.2. Generalized Hoek–Brown rock mass

An elastic–brittle–plastic solution for the axisymmetric problem of a circular tunnel excavated in a generalized Hoek–Brown rock mass can be found in Carranza-Torres (2004), in which the solution is based on a self-similar formulation for the problem. In his formulation, the numerical integration of the second order differential equation is required to get the solution if $a_p \neq 0.5$ and $a_r \neq 0.5$. Here, the example problem appearing in Carranza-Torres (2004) is solved by use of the proposed method and both the results have been compared. In addition, the strain-softening solutions by the proposed method for three different γ^{p^*} are also investigated.

Fig. 6 shows the distributions of radial displacement and stresses calculated by both approaches and also shows the

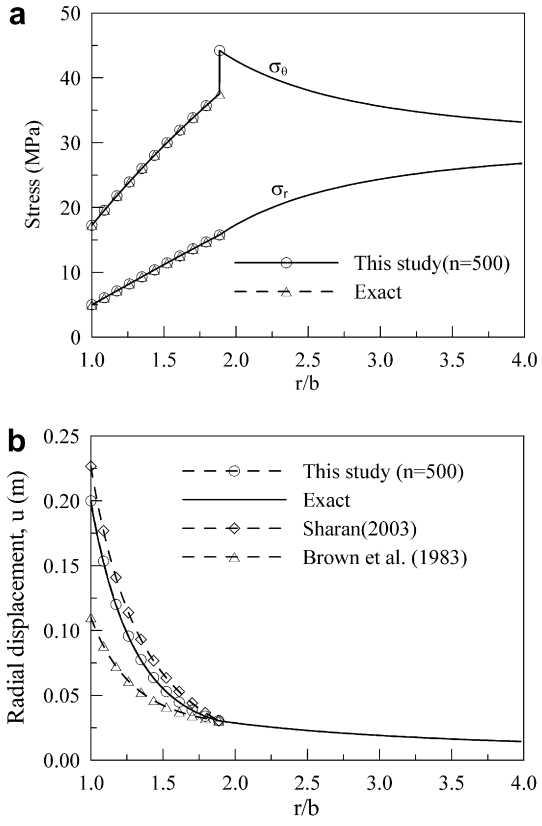

Fig. 5. Comparison of elastic–brittle–plastic solutions for Hoek–Brown rock mass with $\varphi_r = 30°$. Other input data are the same as in Fig. 4: (a) radial and hoop stresses; (b) radial displacements.

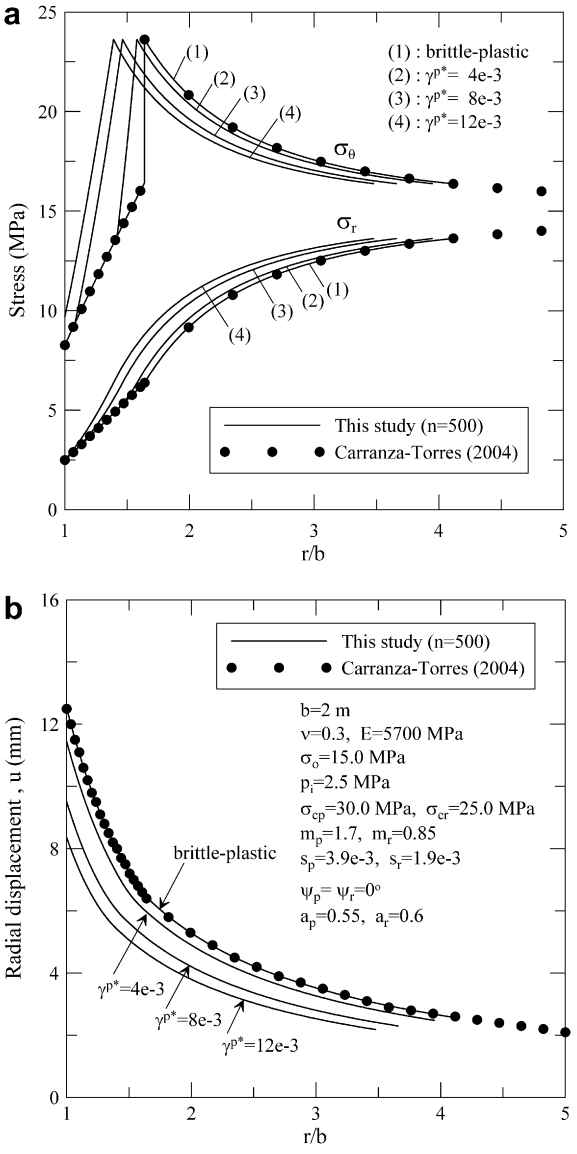

Fig. 6. Elastic–brittle–plastic and strain-softening behavior of a circular opening in a generalized Hoek–Brown rock mass: (a) distribution of radial and hoop stresses; (b) radial displacement.

input parameters for this problem. It should be noted that a_r (=0.6) is larger than a_p (=0.5). For the brittle–plastic case, nearly perfect matching can be seen. It is apparent that the strain-softening solution converges to the brittle–plastic solution when the critical deviatoric plastic strain γ^{p^*} becomes smaller, which confirms the validity of the proposed method for the generalized Hoek–Brown medium. The critical support pressure p_{ic} was calculated numerically as 6.3785 MPa. The plastic radius R_p is the largest (3.28 m) when the behavior is brittle–plastic, and decreases with increasing γ^{p^*}. The softening-residual interface R_s contracts as well with γ^{p^*}. For $\gamma^{p^*} = 12e-3$, the whole plastic zone is strain-softening, i.e., no residual plastic zone is formed. The radial displacement shows the same tendency, so that it is maximum when the rock mass is brittle–plastic and lessens with γ^{p^*}.

Consequently, these results indicate that taking strain-softening behavior into account yields a smaller plastic zone compared to the brittle–plastic case; also, the strain-softening behavior results in a smaller plastic radius.

4.2. Verifications for Mohr–Coulomb rock mass

4.2.1. Elastic–brittle–plastic behavior

As in the verification problem for Hoek–Brown rock mass, five values of n are chosen to demonstrate how the numerical solutions depend on the different selection of n and two different residual dilation angles are considered. The input data are $b = 5$ m, $\sigma_0 = 3$ MPa, $p_i = 0$ MPa, $E = 10$ GPa, $\nu = 0.2$, $\phi_p = 30°$, $\phi_r = 26°$, $c_p = 0.5$ MPa, $c_r = 0.2$ MPa.

The percentages of error in the radial displacement are displayed in Fig. 7, where the exact solution is taken from Park and Kim (2006). The general trend is similar to the case for Hoek–Brown rock mass, Fig. 4. When $n = 500$, the percentage error at the surface of opening ($r/b = 1$) is 0.388% for $\varphi_r = 0°$ and 1.316% for $\varphi_r = 30°$, which means that if $n \geqslant 500$, the calculated displacement is close enough to the exact ones. This figure also hints that the error for the same n becomes larger when the rock mass is more dilatant.

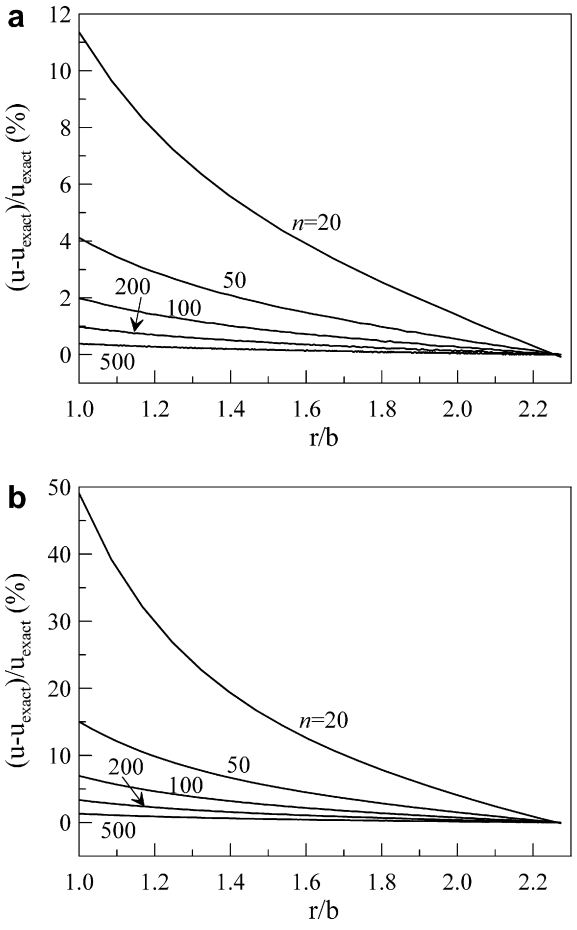

Fig. 7. Approximation errors in radial displacements for a circular opening excavated in Mohr–Coulomb rock mass; $b = 5$ m, $\sigma_0 = 3$ MPa, $p_i = 0$ MPa, $E = 10$ GPa, $v = 0.2$, $\phi_p = 30°$, $\phi_r = 26°$, $c_p = 0.5$ MPa, $c_r = 0.2$ MPa: (a) $\varphi_r = 0°$; (b) $\varphi_r = 30°$.

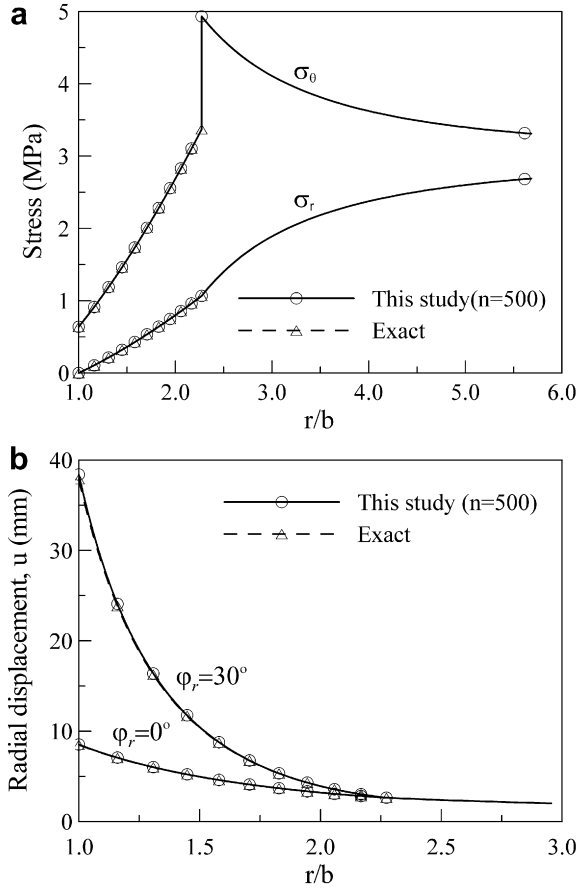

Fig. 8. Stress and radial displacement distributions in Mohr–Coulomb rock mass for. The same input data as in Fig. 7 are used: (a) radial and hoop stresses ($\varphi_r = 30°$); (b) radial displacements ($\varphi_r = 0°$ and $\varphi_r = 30°$).

The calculated distributions of stress and radial displacement for $n = 500$ are plotted in Fig. 8 together with the exact solutions. As this figure indicates, the numerical results are so close to the exact ones that the curves are nearly overlapped. Since $p_i = 0$, the radial stress is zero on the surface of the opening, while the hoop stress is predicted as 0.640 MPa when $\varphi_r = 30°$. The radial displacement on the excavation surface is 38.409 mm for $\varphi_r = 30°$, which is about 4.5 times the value (8.537 mm) for $\varphi_r = 0$.

4.2.2. Strain-softening behavior

The performance of the proposed finite difference scheme in strain-softening regime for M–C rock mass was verified through the construction of ground reaction curve for a circular tunnel excavated in a strain-softening rock. Although their solution process looks rather complicated than the present method, Alonso et al. (2003) also dealt with the same problem based on self-similarity characteristics of the problem. In this section, both the results were compared.

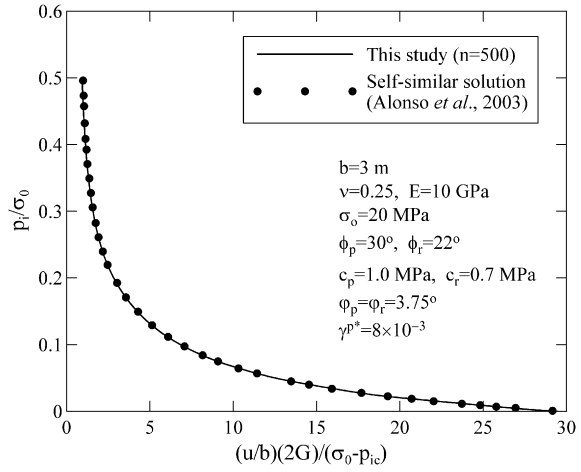

Fig. 9. Ground reaction curve for a strain-softening M–C rock mass.

The ground reaction curve is plotted in Fig. 9 and the evolution of the radii of the elastic–plastic and softening-residual interfaces, which are denoted R_p and R_s, respectively, are shown in Fig. 10. The solid lines indicate the results from the proposed finite difference approximation with $n = 500$, whereas the solid points, which is digitized

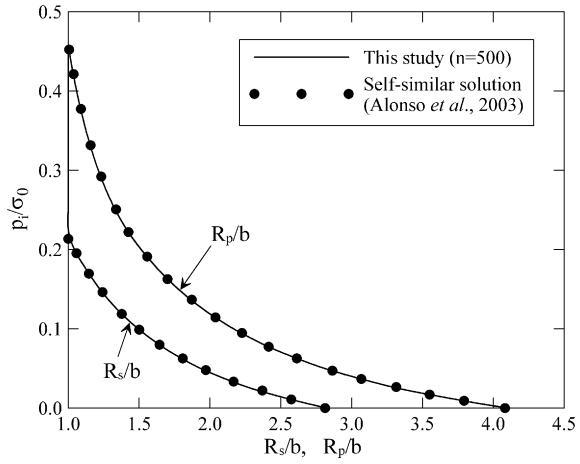

Fig. 10. Evolution plastic radii in a strain-softening M–C rock mass.

from the graphs given in the article by Alonso et al. (2003), represent the self-similar solution. The input parameters, included in Fig. 9, are equivalent to those used by Alonso et al. For this example, the critical support pressure is calculated as $p_{ic} = 9.134$ MPa. Very close agreement can be seen, so that it confirms that the proposed scheme works correctly for the strain-softening regime for M–C rock mass.

4.3. Discussion on the calculation time

In this study, the proposed numerical scheme was implemented in a code written in Fortran90 language. When the code is executed on a desktop computer having Pentium 4 CPU of 2.4 GHz clock speed, the runtime required to get each solution presented in Section 4 is only 15.6 ms for $n = 500$. It should be noted that the sufficiently accurate result was obtained with $n = 500$. Furthermore, the runtime for $n = 5000$ was 62.5 ms, still far less than 1 s. Hence the proposed numerical scheme is very economical from the point of calculation time and does not present a computational burden while giving very accurate results.

5. Influence of the strength parameter '*a*' on the elasto-plastic solution of the generalized H–B rock mass

Although Alonso et al. (2003) tried to get their self-similar solution for the strain-softening behavior of the original H–B rock mass where $a = 0.5$, so far there has been no general strain-softening solution even for the original H–B rock mass as far as authors know. The proposed finite difference scheme, however, takes the generalized H–B criterion into account. Moreover, our approach is most general in that any strength parameter appearing in the criterion can be depend on the internal plastic variable, which is assumed to be γ^p in his study. In the proposed method, the strength parameters required for the elasto-plastic analysis of the generalized H–B rock mass are $m(\gamma^p)$, $s(\gamma^p)$, $\varphi(\gamma^p)$, $\sigma_c(\gamma^p)$, $a(\gamma^p)$ and γ^{p^*}. For simplicity, the single value of γ^{p^*} is chosen here, although each parameter can have its own value of γ^{p^*} if it is supported by the experiments. While restricted to the original H–B rock mass and considered only elastic–brittle–plastic or elastic–perfectly plastic behaviors, many previous works have discussed in detail the influence of such strength parameters as m, s, φ, and γ^{p^*} (Alejano and Alonso, 2005; Alonso et al., 2003; Park and Kim, 2006; Sharan, 2003, 2005; Carranza-Torres and Fairhurst, 1999), so that their roles in the plastic calculation are relatively well understood.

In the latest version of H–B criterion (Hoek et al., 2002), the strength parameter 'a', appearing as the power term in Eq. (5), is no more fixed to 0.5, but it varies in accordant with the geological conditions. Hoek et al. (2002) proposed the following empirical relation for a:

$$a = \frac{1}{2} + \frac{1}{6}\left(e^{-GSI/15} - e^{-20/3}\right) \tag{36}$$

where GSI is the geological strength index reflecting the degree of fracturing and the condition of fracture surfaces of rock mass (Hoek et al., 1995). Considering that GSI is in the range of 10–100, a can take a value between 0.5 and 0.6. For the proper usage of the criterion, therefore, it is necessary to figure out how the elasto-plastic behavior is influenced by the strength parameter a.

In this section, we investigate the influence of the strength parameter a on the ground reaction curves and the development of the plastic zone. Fig. 11 shows four ground reactions curves obtained from the different assumptions on a. Three curves among them postulate that the peak and residual values of a are equal to 0.5, 0.55, and 0.6 respectively, whereas for one of them, a in the strain-softening region varies continuously from 0.5 to 0.6 with γ^p as explained in Eq. (9). Other input data indicated in Fig. 11 remained constant. The difference in the shape of those curves looks substantial, especially when p_i is very low. The curve for continuously varying a is close to that for $a_p = a_r = 0.6$, this is because the thickness of the

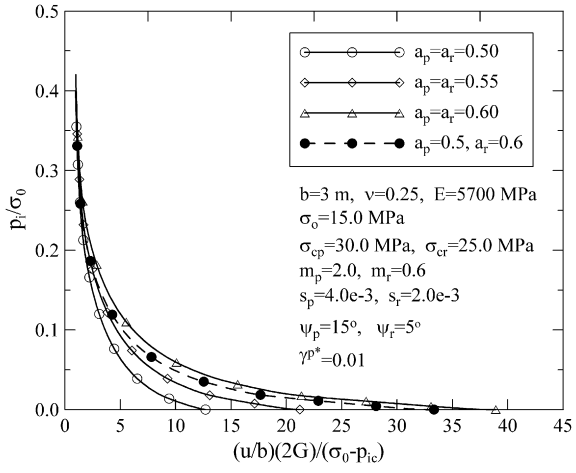

Fig. 11. Ground reaction curves for various 'a' values. The generalized H–B rock mass showing strain-softening.

strain-softening zone in this problem is very narrow as is inferred in Fig. 12 where the radial and hoop stresses for $p_i = 0$ are displayed. The open circles on the curves for σ_r indicate the transition points to strain-softening and residual regimes. If the softening zone is very thin compared to residual zone, the plastic behavior is shifted rapidly to the residual regime. Larger value of a means that the rock mass becomes unfavorable, so that it can be anticipated that the plastic radius grows with increasing a. This tendency is apparent in Fig. 12. The evolution of the plastic radius R_p and the softening radius R_s is plotted in Fig. 13, where the expansion of the plastic zone with a is clearly shown. Fig. 14 shows the radial displacements for $p_i = 0$ on the surface of the opening when $a_p = a_r = a$ is varied between 0.5 and 0.6. The critical support pressure p_{ic} is also plotted in this figure. Recall that no plastic zone is formed for the support pressure larger than p_{ic}. The displacement increases steeply with a, while p_{ic} increases almost linearly. According to this figure, the displacement for $a = 0.6$ is about 3 times larger than that for $a = 0.5$. Judging from the discussion given in this section, the influence of the strength parameter a on the plastic behavior of the generalized H–B rock mass seems considerable. The results presented in this section suggest that the selection of the value for a should be very cautious.

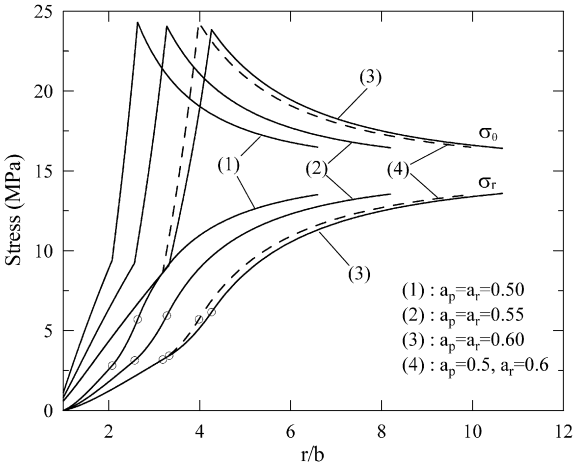

Fig. 12. Distribution of radial and hoop stresses for different values of 'a'. $p_i = 0$.

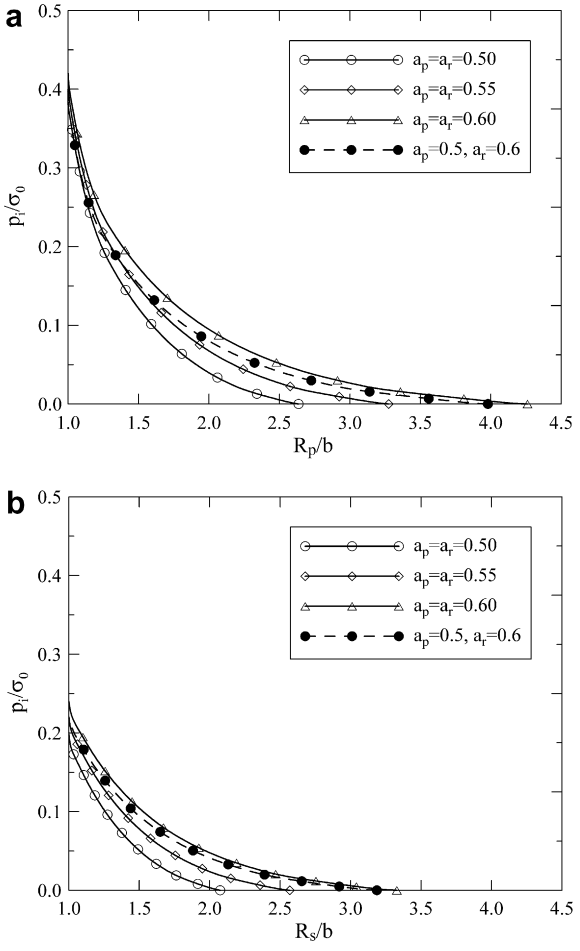

Fig. 13. Evolution of plastic radii for different values of 'a': (a) the plastic radius, R_p; (b) the softening radius, R_s.

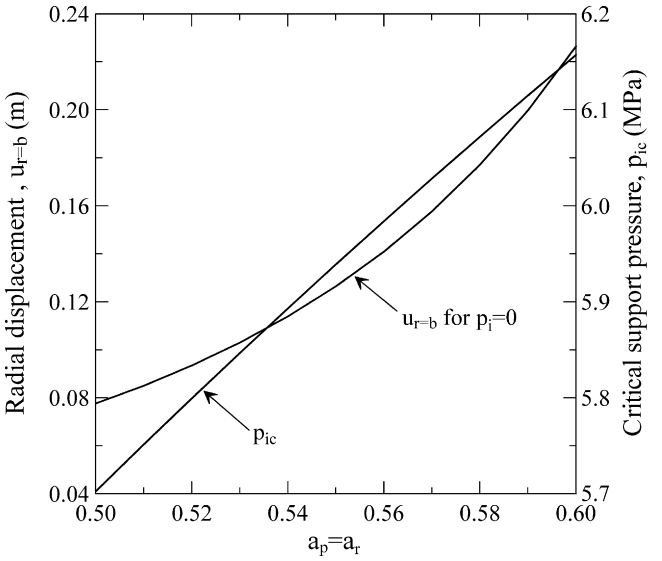

Fig. 14. Radial displacements on the opening surface and the critical support pressure.

6. Summary and conclusions

In this work, a simple numerical procedure for approximating the strain-softening behavior of a circular opening excavated in Hoek–Brown or Mohr–Coulomb medium was introduced. In the proposed method, the plastic ring that forms around the opening was divided into a number of small annuli having non-uniform thickness. Since the radial stress σ_r is decreasing monotonically and the stress values at both the elastic–plastic interface and the excavation surface are known *a priori*, a linear differential decrease in radial stress was assumed in each annulus starting from the outmost one. The corresponding circumferen-

tial stress σ_θ was then determined by enforcing the yield criterion. The size of each annulus was subsequently determined from the finite difference approximation of equilibrium equation. Elastic strain increments in each annulus were calculated from the corresponding stress increments by invoking the Hooke's law. Plastic strain increments in each annulus were obtained from the finite difference approximation of the compatibility equation. The proposed methodology can be used for a perfectly plastic and brittle–plastic material as well as the strain-softening behavior. It is recognized that the strain-softening is attributed here to the *material* behavior, which is certainly a limitation. In general, strain-softening is the effect of localization of deformation and the extension of the present approach to include this effect is currently under investigation.

The proposed method was verified through some illustrative examples. For the brittle–plastic behavior, for which closed form solutions exist, the present method proved to be quite accurate in predicting the stresses and displacements around the circular opening. It was demonstrated that the errors involved are insignificant provided that the plastic zone is divided into a sufficiently large number of annuli.

In the simulations incorporating strain-softening behavior, parametric studies were carried out in the course of specifying the ground reaction curves (GRC) and investigating the locations of plastic radii. For M–C rock mass, the approximate solutions showed perfect matches with the published rigorous solutions. For the generalized H–B rock mass, the strain-softening solution by the proposed method approached the rigorous elastic–brittle–plastic solution with decreasing γ^{p^*}, so that the performance on H–B rock mass could be confirmed. The results clearly showed that more accurate prediction of displacements in rock masses is possible by incorporating strain-softening model and the displacements could be overestimated by assuming the brittle–plastic behavior.

As an application example, the reaction of the elasto-plastic solutions on the variation of the strength parameter '*a*', which is the exponent in the generalized H–B rock mass, was investigated. The results clearly showed that the radial displacements around the opening become larger with the increment of '*a*' and also revealed that the plastic radii grow with '*a*'.

The proposed numerical procedure has been programmed into a FORTRAN code and run on a personal computer having Pentium 4 processor. When the plastic zone is divided into 500, the computing time was far below 1 s, so that the proposed method also seems to be very economical from the view point of calculation time.

Acknowledgements

This work was financially supported by the Kunsan National University's Long-term Overseas Research Program for Faculty Member in the year 2006. In addition, the authors thank the editor and the anonymous reviewers for their valuable comments.

Appendix A. Calculation procedure for the elastic–plastic behavior of a circular opening

Input data

b	radius of a tunnel
σ_0	initial stress in a rock mass existing before the excavation is made
E, v	Young's modulus and Poisson's ratio
p_i	supporting pressure acting on the surface of the tunnel
ω_p, ω_r	peak and residual values of strength parameters

(For Mohr–Coulomb rock mass, ω's represent c, ϕ, and φ, whereas, in Hoek–Brown rock mass, ω's stand for σ_c, m, s, φ, and a)

γ^{p^*}	critical deviatoric plastic strain
n	number of annulus in the plastic zone

Preliminary calculations corresponding to step 0

1. Calculate p_{ic}. If $0 \leqslant p_i < p_{ic}$, then $\sigma_R = p_{ic}$ (If $p_i \geqslant p_{ic}$, no plastic zone is formed, so that elastic solution should be used for whole region).
2. $\Delta\sigma_r = (p_i - \sigma_R)/n$
3. $\sigma_{r(0)} = \sigma_R$; $\sigma_{\theta(0)} = 2\sigma_0 - \sigma_R$
4. $\varepsilon_{r(0)} = (\sigma_R - \sigma_0)/(2G)$; $\varepsilon_{\theta(0)} = (\sigma_0 - \sigma_R)/(2G)$
5. $\varepsilon^p_{r(0)} = 0$; $\varepsilon^p_{\theta(0)} = 0$; $\gamma^p_{(0)} = 0$
6. $\rho_{(0)} = 1$
7. $U_{(0)} = \varepsilon_{\theta(0)}$ $\rho_{(0)} = \varepsilon_{\theta(0)}$
8. $\omega_{(0)} = \omega_p$

Sequence of calculation for each annulus in the plastic zone

1. $\sigma_{r(i)} = \sigma_{r(i-1)} + \Delta\sigma_r$; $\bar{\sigma}_{r(i)} = (\sigma_{r(i)} + \sigma_{r(i-1)})/2$
2. $H_{(i)} = H(\sigma_{r(i)}, \gamma^p_{(i-1)})$; $\overline{H}_{(i)} = H(\bar{\sigma}_{r(i)}, \gamma^p_{(i-1)})$
3. $\sigma_{\theta(i)} = \sigma_{r(i)} + H_{(i)}$
4. $\Delta\sigma_{r(i)} = \Delta\sigma_r$; $\Delta\sigma_{\theta(i)} = \sigma_{\theta(i)} - \sigma_{\theta(i-1)}$
5. $\rho_{(i)} = \rho_{(i-1)}(2\overline{H}_{(i)} + \Delta\sigma_{r(i)})/(2\overline{H}_{(i)} - \Delta\sigma_{r(i)})$;
6. $\Delta\rho_{(i)} = \rho_{(i)} - \rho_{(i-1)}$; $\bar{\rho}_{(i)} = (\rho_{(i)} + \rho_{(i-1)})/2$
7. $\begin{Bmatrix} \Delta\varepsilon^e_{r(i)} \\ \Delta\varepsilon^e_{\theta(i)} \end{Bmatrix} = \frac{1}{2G}\begin{bmatrix} 1-v & -v \\ -v & 1-v \end{bmatrix}\begin{Bmatrix} \Delta\sigma_{r(i)} \\ \Delta\sigma_{\theta(i)} \end{Bmatrix}$
8. $k_{(i-1)} = (1 + \sin\varphi_{(i-1)})/(1 - \sin\varphi_{(i-1)})$
9. $\Delta\varepsilon^p_{\theta(i)} = \left(-\frac{\Delta\varepsilon^e_{\theta(i)}}{\Delta\rho_{(i)}} - \frac{1}{2G}\frac{\overline{H}_{(i)}}{\bar{\rho}_{(i)}} - \frac{1}{\bar{\rho}_{(i)}}\left(\varepsilon^p_{\theta(i-1)} - \varepsilon^p_{r(i-1)}\right)\right) \Big/ \times\left(\frac{1}{\Delta\rho_{(i)}} + (1 + k_{(i-1)})\frac{1}{\bar{\rho}_{(i)}}\right)$
10. $\Delta\varepsilon^p_{r(i)} = -k_{(i-1)}\Delta\varepsilon^p_{\theta(i)}$
11. $\varepsilon^p_{r(i)} = \varepsilon^p_{r(i-1)} + \Delta\varepsilon^p_{r(i)}$; $\varepsilon^p_{\theta(i)} = \varepsilon^p_{\theta(i-1)} + \Delta\varepsilon^p_{\theta(i)}$
12. $\varepsilon_{r(i)} = \varepsilon_{r(i-1)} + \Delta\varepsilon^e_{r(i)} + \Delta\varepsilon^p_{r(i)}$;
    $\varepsilon_{\theta(i)} = \varepsilon_{\theta(i-1)} + \Delta\varepsilon^e_{\theta(i)} + \Delta\varepsilon^p_{\theta(i)}$
13. $\gamma^p_{(i)} = \gamma^p_{(i-1)} + (\Delta\varepsilon^p_{\theta(i)} - \Delta\varepsilon^p_{r(i)})$

14. $U(i) = \varepsilon_{\theta(i)}\rho_{(i)}$
15. If $(0 < \gamma^{p} < \gamma^{p^*})$, then $\omega_{(i)} = \omega_p - (\omega_p - \omega_r)(\gamma^{p}_{(i)}/\gamma^{p^*})$. If $(\gamma^{p} \geqslant \gamma^{p^*})$, then $\omega_{(i)} = \omega_r$

Repeating above 15 steps n times, then $\sigma_{r(n)} = p_i$ and $\rho_{(n)} = b/R_p$, so that $R_p = b/\rho_{(n)}$. The radial displacement at each position is given by $u(i) = U(i)R_p$.

References

Alejano, L.R., Alonso, E., 2005. Consideration of the dilatancy angle in rocks and rock masses. Int. J. Rock Mech. Min. Sci. 42, 481–507.

Alonso, E., Alejano, L.R., Varas, F., Fdez-Manin, G., Carranza-Torres, C., 2003. Ground response curves for rock masses exhibiting strain-softening behavior. Int. J. Numer. Anal. Meth. Geomech. 27, 1153–1185.

Brady, B.H.G., Brown, E.T., 1993. Rock Mechanics for Underground Mining. Chapman & Hall.

Brown, E.T., Bray, J.W., Ladanyi, B., Hoek, E., 1983. Ground response curves for rock tunnels. J. Geotech. Eng., ASCE 109, 15–39.

Carranza-Torres, C., 1998. Self similar analysis of the elastoplastic response of underground openings in rock and effects of practical variables. Ph.D. Thesis, University of Minnesota.

Carranza-Torres, C., 2004. Elasto-plastic solution of tunnel problems using the generalized form of the Hoek–Brown failure criterion. Int. J. Rock Mech. Min. Sci. 41, 480–481.

Carranza-Torres, C., Fairhurst, C., 1999. The elasto-plastic response of underground excavations in rock masses that satisfy the Hoek–Brown failure criterion. Int. J. Rock Mech. Min. Sci. 36, 777–809.

Duncan Fama, M.E., Trueman, R., Craig, M.S., 1995. Two- and three-dimensional elasto-plastic analysis for coal pillar design and its application to highwall mining. Int. J. Rock Mech. Min. Sci. & Geomech. Abstr. 32, 215–225.

Florence, A.L., Schwer, L.E., 1978. Axisymmetric compression of a Mohr–Coulomb medium around a circular hole. Int. J. Numer. Anal. Meth. Geomech. 2, 367–379.

Guan, Z., Jiang, Y., Tanabasi, Y., 2007. Ground reaction analyses in conventional tunneling excavation. Tunnel. Undergr. Space Technol. 22, 230–237.

Hoek, E., Brown, E.T., 1980. Underground Excavation in Rock. Institution of Mining and Metallurgy, London.

Hoek, E., Kaiser, P.K., Bawden, W.F., 1995. Support of Underground Excavations in Hard Rock. Balkema, Rotterdam.

Hoek, E., Carranza-Torres, C.T., Corkum, B., 2002. Hoek–Brown failure criterion – 2002 edition. In: Proceedings of the 5th North American Rock Mechanics Symposium and 17th Tunnelling Association of Canada Conference, Toronto, pp. 267–273.

Park, K.-H., Kim, Y.-J., 2006. Analytical solution for a circular opening in an elasto-brittle-plastic rock. Int. J. Rock Mech. Min. Sci. 43, 616–622.

Press, W.H., Teukolsky, S.A., Vetterling, W.T., Flannery, B.P., 1992. Numerical Recipes in Fortran. Cambridge University Press.

Sharan, S.K., 2003. Elasto-brittle-plastic analysis of circular opening in Hoek–Brown media. Int. J. Rock Mech. Min. Sci. 40, 817–824.

Sharan, S.K., 2005. Exact and approximate solutions for displacements around circular openings in elastic–brittle–plastic Hoek–Brown rock. Int. J. Rock Mech. Min. Sci. 42, 542–549.

Timoshenko, S.P., Goodier, J.N., 1982. Theory of Elasticity. McGraw-Hill Book Co.

Varas, F., Alonso, E., Alejano, L.R., Fdez-Manin, G., 2005. Study of bifurcation in the problem of unloading a circular excavation in a strain-softening material. Tunnel. Undergr. Space Technol. 20, 311–322.

Wang, Y., 1996. Ground response of circular tunnel in poorly consolidated rock. J. Geotech. Eng., ASCE 122, 703–708.